D36

In-process Image Detecting Techniqu for Determination of Overlay, and Image Quality f r ASM-L Waf r Stepper

R. Pforr, S. Wittekoek*, R. Van Den Bosch, L. Van den hove, R. Jonckheere, T. Fahner*, R. Seltmann**

IMEC Leuven, Kapeldreef 75, B-3001, Belgium
SW,TF: ASM Lithography BV, Meierijweg 15, 5503 HN Veldhoven, The Netherlands
RS: Fraunhofer Institut fuer Mikroelektronische Schaltungen und Systeme, Institutsteil Dresden, D-O 8080, Grenzstraße 28

ABSTRACT

The possibilities of in-process blue image sensing by using only the implemented darkfield TTL alignment system of a stepper are investigated. It is shown, that all overlay related parameters of a PAS5000/50 and /70 stepper such as red-blue, magnification, rotation and translation can be measured from an enhanced latent image in a special dyed resist but also with some reduction in accuracy in a pure resist only. Results of overlay measurements on typical technological layers and of similar experiments based on latent image sensing in dyed and in pure resist are given, indicating the capability of in-situ overlay control and correction on process wafers. A new *alignment target sensing* (ATS) technique of focus measurement using the alignment detection system of the stepper for both daily focus control and correction as well as for focus setting on process wafers with typical technological layers is introduced. The method uses special designed alignment markers containing lines and spaces at the working resolution. Results are given for sensing the developed resist pattern as well as the latent image for an i-line and a DUV stepper. The applicability is demonstrated by measuring the influence of varying resist layer thickness and of varying oxide layer thickness of various film stacks of technological layers on optimum focus. The validity of these results is proven by comparisons to other focus measurement techniques such as chessboard and SEM linewidth measurements. A mathematical model based on the diffraction theory of thin gratings has been developed to support the marker design as well as to calculate the Image Quality Signal (IQS) vs. focus/exposure curves of developed images. The model has been verified by experiments.

1. INTRODUCTION

New high numerical aperture lenses with reduced projection wavelength have demonstrated the possibility of printing resist feature sizes in the deep sub-micron region [1,2]. This will require a significant reduction of budgets for overlay, focus, and exposure variation in comparison to the present state-of-the-art in production lines. A tighter control of all factors influencing the image printing quality, especially the technological related ones, will become more and more of interest. Therefore techniques have been developed to check the printing quality of the stepper by sensing and characterizing the latent image (on test wafers) and conclude stepper set-up parameters already before exposing of production wafers [3,4]. Until now this is done by using additional measurement instruments outside of the stepper. A significant improvement would be achieved when it becomes possible to detect and set-up quickly and accurately the most important stepper parameters in the stepper immediately before exposing the wafers with a production mask. Parameters to be considered are best focus, blue image tilt, overlay error, and incoupled energy. Goal of the investigations has been to determine, whether it is possible to do such an in-process control with the darkfield TTL alignment system implemented in the ASM-L PAS5000 steppers without any hardware modifications. Regarding the focus determination the present work has concentrated on developed images in resist mainly, but the usability of latent images is demonstrated in principle and will be pursued in the near future. For in-process overlay control procedures the work was consequently related to latent images in non-dyed and specifically dyed resists [5]; developed features were used only for accuracy comparisons.

2. Theoretical background of *A*lignment *T*arget *S*ensing (*ATS*)

In contrast to most other wafer steppers ASM-L's PAS series use an alignment system which is intended to

0-8194-0829-8/92/$4.00

suppress wafer related technological influences such as resist thickness variations across the marker and changes of the optical quality of technological layers across the marker on alignment accuracy by a spatial filtering technique shown schematically in Fig. 1. Only the plus/minus first order diffracted waves of a phase grating marker are used to detect the marker position relative to the reticle by a direct through-the-lens alignment system. Because of the darkfield illumination principle the signal-to-noise-ratio of the alignment detection system is large. As well known even diffraction efficiencies of standard grating markers of approximately one percent are large enough to get good alignment accuracy [6]. Therefore a detection of small signal variations due to small exposure induced optical changes in resist by the alignment system could in principle be expected to be possible. One of the goals was to prove the possibilities of in-process (and even in-situ) control and correction of the exposed marker position on processed wafers.

To determine best focus by sensing the contrast of a latent image in resist by use of this alignment system is more complicated. The optical filtering at low spatial frequencies, which is an advantage for alignment marker sensing, is a disadvantage for the focus and contrast detection, since these parameters are sensitive only at high spatial frequencies near the working resolution of the lens. Therefore the marker design has to be changed in such a way, that exposing an alignment target in resist with varying contrast results in a change of the intensity of the diffracted light in the plus/minus first orders of the fundamental grating. For better understanding of the processes the theoretical background of the technical principle is explained first.

A typical marker design is shown in Fig. 1. The coarse and fine grating consist of a rectangular transmittance distribution. The transparent homogeneous lines of the primary marker (with a fundamental coarse grating frequency of f) are substituted by a fine grating with the frequency ν near the lens resolution limit. The projection of such a grating onto the wafer with a lens can be approximately described by:

$$I'(x') = 0.5*I'_0\,\{0.5+(2/\pi)*\{\sum_{p=0}^{\infty} K[(2p+1)\nu,\Delta z]*\sin[2\pi\nu(2p+1)x']/(2p+1) + \sum_{q=0}^{\infty} K[(2q+1)f,\Delta z]*\sin[2\pi f(2q+1)x]/(2q+1)\}$$

$$+(2/\pi)^2 * \sum_{p=0}^{\infty}\sum_{q=0}^{\infty} \{K(\omega_{pq},\Delta z)*\cos[2\pi\omega_{pq}x'] - K[\omega_{pq},\Delta z]*\cos[2\pi\omega_{pq}x']\}/(2p+1)(2q+1)\} \qquad (1)$$

$$\text{with} \quad \omega^{\pm}_{pq} = (2p+1)\,\nu \mp (2q+1)\,f. \qquad (2)$$

$K(\omega, \Delta z)$ is the contrast transfer function of a rectangular grating during marker exposure.
Due to the development of resist a local resist thickness variation d(x) is formed, which is given by the intensity distribution $I'(x')$ (I'_0 is the open frame light intensity on the wafer level), exposure time t_B and the characteristic curve of resist ($d(x) = d_0 - D * I'(x') * t_B$ for the linear part of curve; for the calculation is used d_0 = 1366 nm, D = 7.7 nm* cm^2/mJ).
During alignment detection the marker is illuminated perpendicularly so that the reflected wave gets a phase shift $\phi(x') = 4*\pi* d(x')*(n-1)/\lambda$ (n refractive index). Its complex amplitude is given by

$$\hat{A}_R(x') = C * \exp(i\,\phi(x')) = \hat{C} * F_1 * F_2 * F_3 * F_4 \qquad (3)$$

with

$$F_1 = \sum_{q_1=-\infty}^{\infty} J_{q1}[\phi_1 K[(2q_1+1)\nu,\Delta z]/\pi]*\exp[2\pi i q_1 \nu x'] \qquad (3.1)$$

$$F_2 = \prod_{p_2=0}^{\infty} \{\sum_{q_2=-\infty}^{\infty} J_{q2}[\phi_1 K[(2q_2+1)\nu,\Delta z]/((2p_2+1)*\pi)]*\exp[2\pi i q_2(2p_2+1)fx']\} \qquad (3.2)$$

$$F_3 = \prod_{p_3=0}^{\infty} \{\sum_{q_3=-\infty}^{\infty} (i)^{q3}*J_{q3}[2*\phi_1*K[\nu-(2p_3+1)f,\Delta z]/((2p_3+1)*\pi^2)]*\exp[2\pi i(\nu-(2p_3+1)f)q_3x']\} \qquad (3.3)$$

$$F_4 = \prod_{p_4=0}^{\infty} \{ \sum_{q_4=-\infty}^{\infty} (i)^{q4} * J_{q4}[2*\phi_1 * K[\nu+(2p_4+1)f,\Delta z]/((2p_4+1)*\pi^2)]*\exp[2\pi i(\nu+(2p_4+1)f)q_4x']\} \quad (3.4)$$

with $\phi_1 = 4*\pi* D *I_0'*t_B/\lambda$, whereas the approximation $K[(2p+1)\nu,\Delta z] = 0$ $(p\geq 1)$ has been applied. $J_{\pm q}()$ are Bessel functions of order $\pm q$.
A coefficient comparison of $\hat{A}_R$ with respect to $\exp(\pm 2\pi i f x')$ gives the amplitude of the ± 1st order diffracted wave, which is passing the frequency filtering diaphragm, creating a light intensity on mask level, which is proportional to $(A_{-1}+ A_{+1})(A^*_{-1}+ A^*_{+1})$. The IQS, being measured by the alignment system of the stepper, is proportional to $(A^*_{-1} A_{+1}+A_{-1}A^*_{+1})$. For the amplitudes A_{+1} and A_{-1} the coefficient comparison gives an expression which is extremely complex. To simplify matter the Bessel functions of higher order are suppressed, and the approximations $K[(2p+1)f]=1$ $(p\geq 1)$ and $K[\omega_{pq},\Delta z]=K[(2q+1)\nu,\Delta z]$ are applied. The light intensity resulting in the image quality signal is given by the formula :

$$I_{IQS} = I'_0 * 2 * \{J_0(\Phi_{1m})*F_{21}\}^2*\{/F_{s1}/^4 + F_{s0}^4\} \quad (4)$$

with

$$F_{21} = J_0(\Phi_3)*\{J_1(\Phi_0)*\{J_0(\Phi_1)*J_0(\Phi_2)+J_1(\Phi_1)*J_1(\Phi_2)] + J_2(\Phi_0)*J_1(\Phi_1)*J_0(\Phi_2)-J_0(\Phi_0)*J_2(\Phi_1)*J_1(\Phi_2)\} \quad (4.1)$$

$$/F_{s1}/ = J_1(\phi_{0m})*J_0(\phi_{1m})*J_0(\phi_{2m})*J_0(\phi_{3m}) \quad (4.2)$$

$$F_{s0} = J_0(\phi_{0m})*J_0(\phi_{2m})*J_0(\phi_{2m})*J_0(\phi_{3m}) \quad (4.3)$$

$$\Phi_p = (\phi_1/\pi)/(2p+1) \quad (4.4)$$

$$\phi_{qm} = (\phi_1/2)*(2/\pi)^2*K[\nu,\Delta z]/(2q+1) \quad (4.5)$$

$$\Phi_{1m} = (\phi_1/\pi)*K[\nu,\Delta z] \quad (4.6)$$

$$\phi_1 = 4*\pi*D*t_B*I_0'/\lambda. \quad (4.7)$$

It shows clearly, that the light being diffracted in the first orders of the primary grating is dependent on the image contrast $K(\omega,\Delta z)$ of the fine grating during resist exposure.

3. RESULTS

3.1. Image quality sensing

Developed Image

To check the validity of above ideas and related theory, the possibilities of determining focus by alignment signal strength (IQS) measurements has been proven first for developed resist patterns. To get an idea of optimum geometry of the marker, various designs have been checked. Following parameters were varied:
- number of lines per fine grating,
- frequency of the fine grating,
- direction of the lines/spaces of the fine grating,
- sub-division of the gratings in various fine gratings with different frequencies,
- transmittance of the regions of course grating spaces (dark, bright, chessboard),
- moir'e gratings (diffraction enhanced marker),
- sequence of pattern exposure.

In the following only some typical results are given, allowing an understanding of the principle of the technique

and its applicability.

In Fig. 2 the IQS versus defocus is shown for a sub-divided fine grating marker (2a) and a so called duty grating marker (2b), i.e. a grating with a large line/space ratio. The curves of both figures represent two fundamental classes of curve shapes, a concave and a convex type. For both marker designs the IQS is strongly dependent on defocus. A well defined extreme value can be determined, corresponding with the highest contrast of latent image of the marker gratings in resist. However for best focus the dependence of IQS on exposure for both marker types is significantly different. The sub-divided fine grating marker type gives a large IQS vs. exposure gradient ($(\partial IQS/\partial H)f_{opt}$), whereas the duty marker type results in a very small IQS vs. exposure gradient, which is shown in Fig. 3 (curve 3 and 4). In this figure the IQS vs. exposure curves of some other marker designs are given also, indicating characteristic differences. Because of its large gradient, curve 3 allows the determination of incoupled energy, provided the best focus is known. Since the IQS variation versus exposure dose is low for curve 4, this marker design allows a focus determination by one ATS measurement only, provided the incoupled energy is known. For curve 1 the exposure dependence of IQS is also high but not well defined (for two exposures one IQS). Curves such as given in Fig. 3 have been used to compare and to do a pre-selection of the most interesting marker designs for detailed investigations.

To determine the accuracy of focus measurements the reproducibility of the IQS vs. focus curves has been measured for the two marker types of Fig. 2. Fig. 4 shows the signal reproducibility for fixed exposures on a single wafer ("one-wafer" reproducibility, i.e. 11*11 array with fixed exposure and varying focus) to be ± 5 percent (sub-divided fine grating) resp. ± 2.5 percent ("duty" grating).
The "wafer-to-wafer" reproducibility of focus measurements (11 wafers with fixed exposure and varying focus) as well as the result of the "single-wafer" case is given in Table 1. Both marker designs show an extremely high reproducibility allowing this technique to be applied for daily focus measurement and set-up of PAS5000 series steppers.

Results of the daily focus measurements of PAS5000/50 based on ATS with two marker designs are shown in Fig. 5. The measurement accuracy of daily focus measurements defined by the average of daily 3-sigma focus variation based on 6 focus values per daily wafer is 0.05 µm for marker (1,-1) and 0.11 µm for marker (-3,-3). As can be seen, both curves have a certain offset, which remains constant. This is due to the resist layer development status. For marker (1,-1) the resist in the exposed regions is only partially developed, which means that best focus (or highest image contrast) is defined in the region near the resist/air interface. For marker (-3,-3) the resist is fully washed away from the substrate surface in the exposed regions; therefore this marker type is referring to the whole resist depth.
The ATS focus result of marker (1,-1) indicates a 3-sigma long term focus stability of the PAS5000/50 of 0.23 µm even in case the value of helium pressure failure is included. In case the failure is omitted, a 3-sigma value of 0.14 µm could be achieved. As shown, the ATS focus variations are in close coincidence with results of chessboard measurements. The difference can be understood by taking into consideration that the resist clearing exposure (peak of the "christmas tree") has been used as focus determining criteria, which refers more to the region of resist/substrate interface.

In a second phase the usefulness of ATS was investigated on technological layers with varying resist layer thickness as well as varying thicknesses of films of various stacks of technological layers.
In Fig. 6 the best focus measured by ATS for marker designs of Fig. 2 is given versus resist thickness, showing approximately a sinusoidal variation. An identical variation has been observed using chessboard focus measurements as well as by measurements based on determination of top/base linewidth ratio (as measured using cd-SEM). This variation is due to a shift of the largest aerial image contrast in the depth of the resist film by changing interference (film thickness) conditions.
The same focus behaviour has been found also for varying oxide thickness on the substrate oxide and on a film stack oxide/nitride shown in Fig. 7a and 7b. No focus shift with varying oxide thickness occurs in case of the film stack oxide/poly (see Fig. 7c) since the 300 nm thick poly-Si film used is non-transparent for the actinic light (365 nm) and no change of interference conditions occurs in this case. However because of the varying interference conditions for the signal measuring light (633 nm), of course, the IQS for best focus is varying (see Fig. 7d).

In IC production lines, due to varying film thicknesses of resist and technological layers, and varying development conditions, the effective energy coupled into the resist resp. the resist development rate is

varying. To apply the ATS technique successfully therefore a certain exposure latitude to do accurate best focus measurement is necessary. Fig. 8 shows the change of focus versus exposure for various oxide thicknesses for the marker design with sub-divided fine gratings. As can be seen there is a large exposure range without significant focus variation. In Table 2 this "exposure latitude" is given for the substrate oxide as well as the latitude of the film stacks oxide/poly and oxide/nitride for a focus change of ± 0.1 µm. As can be seen for all layer stacks the latitude is large enough to get accurate focus results by applying the ATS technique.

The ATS focus determination technique has been tested successfully also for various resists such as dyed and non-dyed IX500/JSR, Mc Dermid's 2015, Shipley's XP3413 and XP89131, and for typical g-line resists. The method has been investigated for both an i-line and a DUV stepper (see Fig. 9).

Latent Image

In comparison to the measurement on developed marker images, the measurement of latent images is much more complicated due to the relatively small changes of refractive index and absorption caused by the exposure. The intensity of the diffracted light is extremely small in the relevant plus/minus first orders of the coarse grating. On the other hand the diffraction has to be understood as diffraction on more or less thick gratings (Q=5...20, where $Q=2*\pi* \nu^2*\lambda*d/n$ is a measure of "optical grating" thickness). Due to the vertical illumination of the marker the reconstruction of this grating is not on Bragg condition. This lowers the efficiency of diffraction too. Therefore, based on the standard IQS measuring procedures, it is hard to get an accurate IQS vs. focus curve allowing a precisely determination of optimum focus.

In case of an AlSiCu substrate the optimum focus of PAS5000/50 could be determined relatively reproducible using marker exposures of JSR's IX500, as indicated in Fig. 10a. The variation of the maximum of the IQS vs. focus curve, which has been derived by curve fitting with polynomials of 2nd order, is small. On other substrates the results are worse. Therefore to get fully satisfying results an improvement of the detection strategy is essential to be successful for substrates with smaller reflectivity.
Comparable results have also been obtained for the DUV stepper PAS5000/70 by using acid hardened resists. The exposed non-baked resist gives no IQS even for extremely high exposures. However by baking a relatively large change of refractive index of the resist in the exposed regions occurs and alignment and consequently IQS measurement becomes possible; in that case relatively well defined IQS vs. focus curves were obtained (see Fig. 10b).

3.2. Overlay

For a standard marker the exposure induced changes especially of the refractive index in a pure resist and absorption in a dyed resist are large enough to allow an alignment on latent marker images. This is the case not only on test wafers but also on wafers with stacks of technological layers. The alignment signal strength is of course dependant on the exposure, the reflectivity of the substrate, and the status of resist (dyed/non-dyed or baked/non-baked, layer thickness etc.), as shown in Fig. 11. Obviously the IQS of a dyed i-line resist is significantly larger than of a non-dyed resist on substrates with reflectivities in the range of silicon and lower, i.e. most of all substrates. The highest IQS is for the DUV resist of acid hardened type (here Shipley's XP89131), but the IQS are larger for pure resist due to the relatively large changes of refractive index in the resist after PEB (140 C, 60') and due to absorption of the alignment light by the additional dye in dyed resist.
But only in case of dyed resist the latent image of a marker (IQS appr. 30%) can be detected and used for in-situ measuring of overlay error and correction of the exposure positions on process wafers by a DUV stepper. In pure XP89131 resist the position of the latent image cannot be measured due to extremely small diffraction efficiency of marker gratings (no alignment and therefore no IQS measurement possible). In contrast, for a typical i-line resist dying is helpful but not essential for allocation of the marker.

A key question for the proposed in-situ overlay control and correction procedure is whether the overlay error measuring accuracy on latent image markers with small IQS is small enough to avoid wrong settings. This has been tested by applying the standard overlay test procedure. Overlay test results with latent image and developed markers are given in Fig. 12 and Table 3.
Fig. 12 indicates that for a non-dyed i-line resist (IX500) the measured overlay error (here given as square root of sum of squares of 3-sigma overlay errors) is decreasing continually with increasing exposure, i.e. increasing IQS of latent marker image, and reaches a saturation accuracy of appr. 90 nm for 700mJ/cm^2. In case of a dyed

i-line resist the measured overlay error is obviously significantly smaller and only a minor random variation of overlay error is measured vs. exposure. As can be seen clearly the developed resist image gives the best results (in case of equal line/space ratio of resist marker grating). The differences are primarily due to IQS differences of markers and have to be considered as a consequence of measurement error differences of the various markers. Assuming a negligible measurement error for the developed marker and the same overlay error for all wafers (same primary marker for stepper alignment before exposing the resist) the additional measurement error due to the small IQS of the latent image marker has been calculated and is plotted vs. exposure in Fig. 12. This error was calculated by $\sqrt{\{[(3\sigma_{x,li})^2+(3\sigma_{y,li})^2]+[(3\sigma_{x,dr})^2+(3\sigma_{y,dr})^2]\}/2}$, whereas the indices "li" and "di" indicate the latent image and developed resist.
All results have been obtained using the standard overlay exposure and measuring procedure, i.e. no special alignment procedures have been used for alignment on latent image marker. It can be expected, that an improvement of the individual measurement accuracy is obtained for latent image markers in case the measuring procedure is modified appropriately, for instance by increasing the number of alignment scans.
The overlay accuracy of the various marker types has been tested also for various stacks of technological layers (see Table 3). Similar accuracy trends have been obtained in principle, but the relative differences are smaller (3-sigma overlay error on markers of developed, and latent image in dyed and in pure resist are related as 52 nm : 58 nm : 62 nm).

The latent marker images in resist have been used also to measure the position difference of the blue and red image by applying the so called "mirror mapping" (matching) procedure. In contrast to the overlay tests, the results given in Table 4 show that the differences between the most interesting red-blue difference determining parameters are very small for latent marker images in pure and dyed resist as well as developed resist. This is due to the averaging of a lot of measurements per exposed field (12 fields were exposed and measured) and because of first layer markers are equal those (etched in silicon). Therefore it can be concluded that a self-calibration of steppers of the PAS5000 series is possible with high accuracy by use of latent marker images only.

4. Conclusions and summary

Fundamentals of an in-process focus measurement technique based on an *alignment target sensing* of an appropriately designed alignment pattern and the alignment system of the steppers of the PAS5000 series without any hardware modifications is introduced. On developed images very good focus measurement reproducibility was achieved for both special test wafers as well as wafers with typical technological process layers. The usability of this focus determining technique was demonstrated also with latent images in resist. To apply the ATS technique for typical i-line resists some minor changes of alignment target sensing software is necessary.
Furthermore the possibility of in-situ overlay control and correction on process wafers is demonstrated. For standard i-line resists only minor software changes to improve the position measurement accuracy is needed to apply such a technique. For acid hardened resists there is an additional need to add a special dye to the resist, since the changes of refractive index and/or absorption of a pure resist are to small for an accurate determination of the marker position. Procedures to improve this are under investigation.

5. Acknowledgements

The authors would like to thank Dr. W. Guenther from Friedrich-Schiller-Universitaet of Jena for preparing the dyes and IMEC for supporting the work.

6. References

1. K. Ronse, R. Jonckheere, K.-H. Baik, M. Goethals, L. Van den hove, "Sub-quarter micron phase-shifting lithography using the DESIRE process at 248 nm (deep UV)", *Microelectronic Engineering*, Vol.17, No.1-4, pp. 69-74, March 1992.
2. K.-H. Baik et.al., "Liquid phase silylation for the DESIRE process", *Abstracts SPIE Microlithography*, p. 90, San Jose, March 1992.

3. T. E. Adams, "Application of Latent Image Metrology in Microlithography", *Proc. SPIE*, Vol. 1464, pp. 294-311, March 1991.
4. K. C. Hickmann, S. M. Gaspar, K. P. Bishop, S. S. H. Naqvi, J. R. McNeil, "Use of diffracted light from latent images to improve lithography control", *Proc. SPIE*, Vol. 1464, pp. 245-257, March 1991.
5. R. Pforr, R. Seltmann, D. Kunze, W. Guenther, D. Faßler, "Contrast enhancement of the resist latent image using exposure induced absorption amplification - fundamentals, modelling, and applicability", *Microelectronic Engineering*, Vol. 17, No.1-4, pp. 321-326, March 1992.
6. S. Wittekoek, J. v. d. Werf, R. A. George, "Phase gratings as wafer stepper alignment marks for all process layers", *Proc. SPIE Optical Lithography IV*, Vol. 538-35, , pp. 24-31, March 1985.

marker type	mean focus/μm	3σ/μm	mean focus/μm	3σ/μm
0.5μm fine grating (convex form)	0.56	0.047	0.62	0.12
0.6μm duty grating (concave form)	0.39	0.078	0.41	0.10

Table 1

Focus measurement reproducability of ATS for developed pattern with marker types of Fig. 2 (column1: 11*11 FEM with constant exposure; column 2: wafer-to-wafer reproducability of 11 wafers)

Substrate	Marker 1	Marker 2
Oxide/nitride	±39%	±25%
Oxide/poly	±32%	±21%
Oxide	±25%	±16%

(Marker 1: sub-divided fine grating; Marker 2: 0.6 μm duty grating)

Table 2

Exposure latitude of ATS (for ±0.1 μm focus measurement accuracy) of developed pattern of markers of Fig. 2

Substrate	Resist	$3\sigma_x$/nm	$3\sigma_y$/nm **	Δv/nm
Oxide/poly	Dye*	59	66	57
"	Pure*	68	62	75
"	Dev.*	63	48	55
Oxide/nitride	Dye	66	58	65
"	Pure	66	66	72
"	Dev.	52	44	49
Oxide	Dye	61	57	63
"	Pure	55	47	76
"	Dev.	58	57	59
AlSiCu	Dye	55	47	58
"	Pure	59	57	62
"	Dev.	50	40	51
AlSiCuTiW	Dye	61	56	70
"	Pure	66	76	77
"	Dev.	54	49	56

(* "Dye" means: dye and IX500; "Pure" means : IX500 only; "Dev." means: developed IX500
** maximum overlay error vector)

Table 3

Short term overlay accuracy of PAS5000/50 on various film stacks of technological layers, measured on latent and developed images of standard marker on dyed and non-dyed resist

Resist	Image	Tx/nm	Ty/nm	Rot./μrad	Magn./nm/cm²	σ_x/nm	σ_y/nm	Tp_x*	Tp_x*
Pure	Latent	9	-16	1.542	-21	33	27	-4	14
Dyed	Latent	1	4	1.366	-27	33	34	-37	45
Pure	Devel.	-2	-17	1.579	-16	31	27	-37	47

(* in nm/cm²)

Table 4

Deviation of blue and red images of PAS5000/50, measured with ASM-L's standard "mirror mapping/red-blue" procedure on etched (1st marker) and latent and developed images (2nd layer) in dyed and non-dyed resists

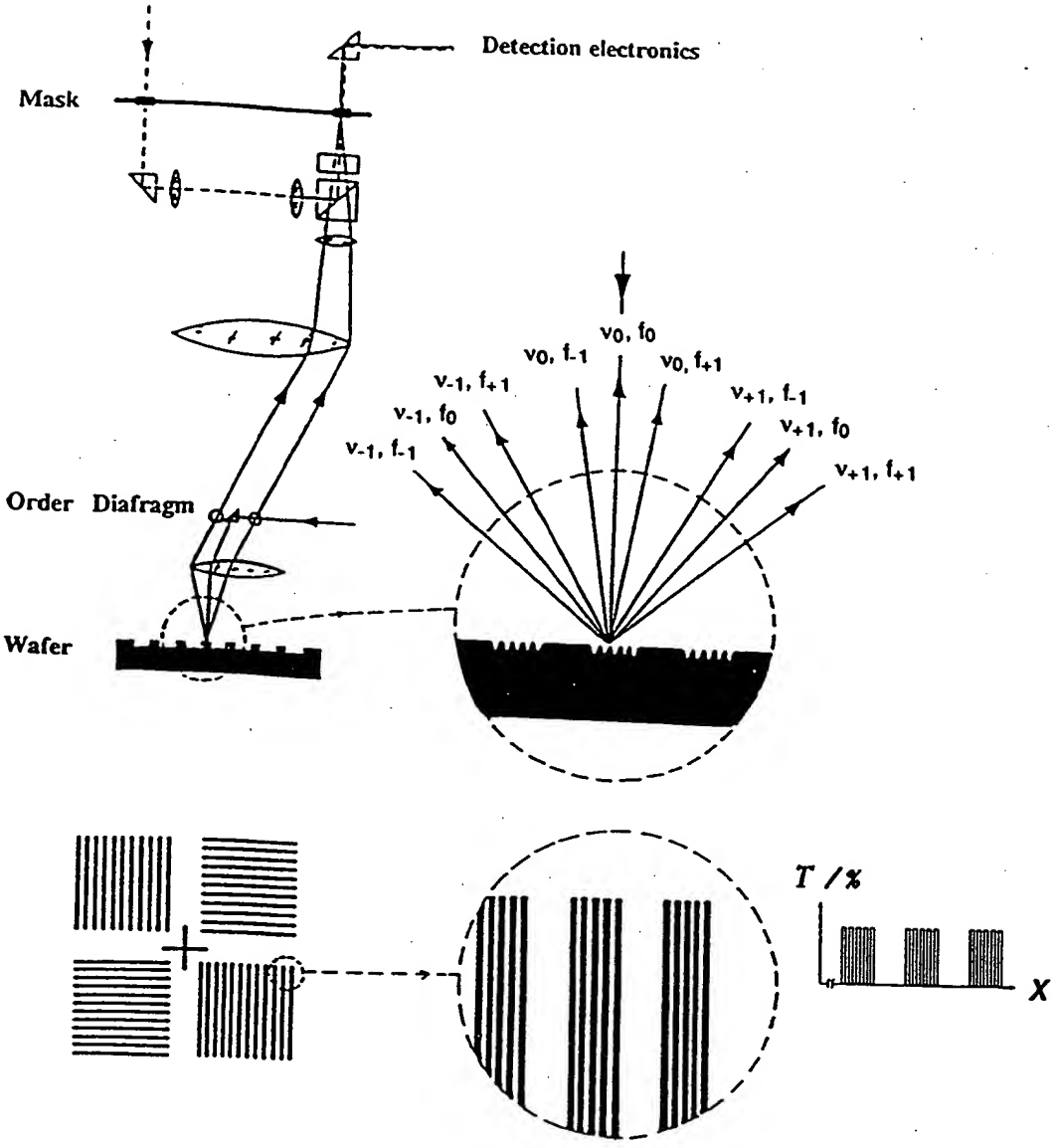

Figure 1.
Alignment target sensing (*ATS*) technique for focus measurement.

(*The standard "coarse" alignment marker is modified by a sub-structure of marker grating lines and spaces consisting of fine gratings with frequencies near the resolution limit. Vertical illumination leads to various diffracted waves having spatial frequencies given by a sum of multiples of the frequency of the coarse and fine grating. The intensity of the diffracted waves depends on the phase modulation caused by both the coarse and fine grating and therefore on the contrast of the aerial image of fine grating during marker exposure. The relative change of intensity of the plus/minus first order diffracted waves of the coarse grating caused by marker exposure with varying focus settings is measured. This results in an Image Quality Signal (IQS) of the stepper as determined using the alignment system.*)

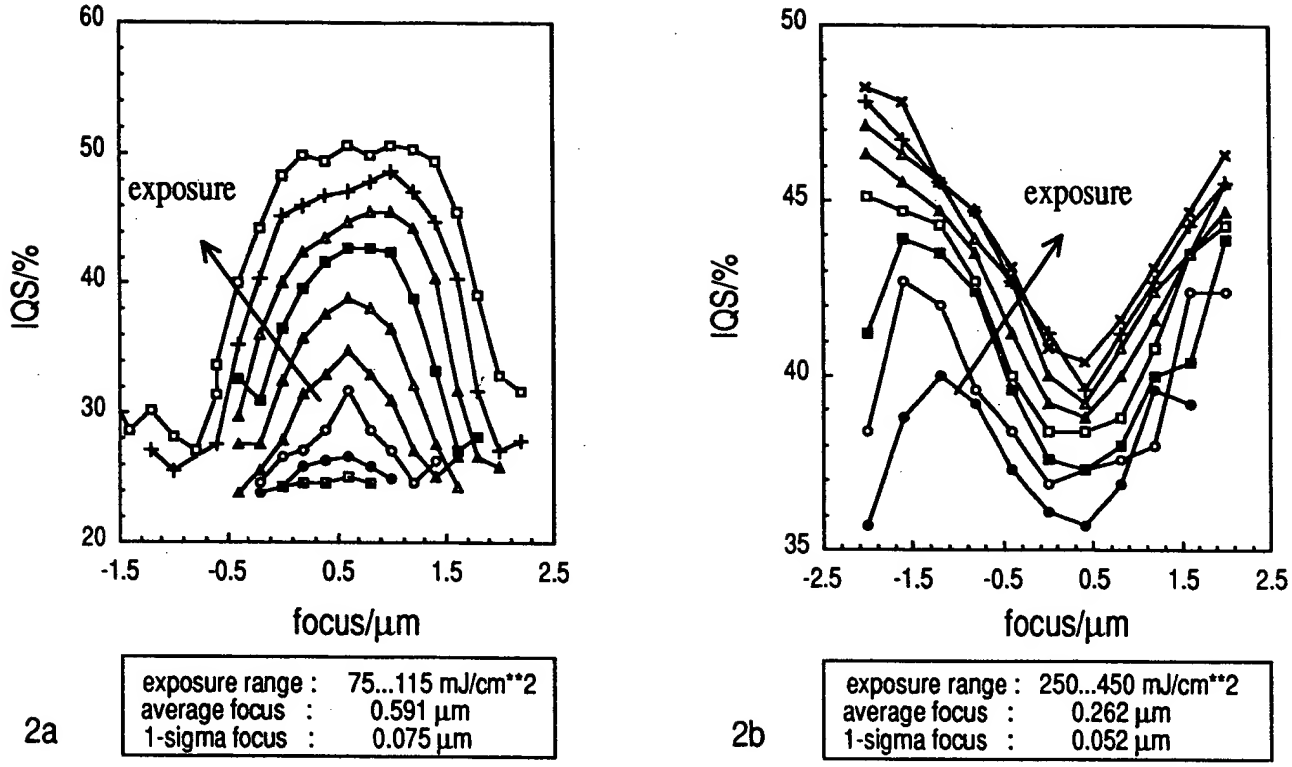

Figure 2. IQS vs. focus/exposure for a sub-divided fine grating (a) and a grating with large line-space-ratio (b), measured for developed patterns with ASM-L's PAS5000/50 and JSR's IX500 on Si-substrate

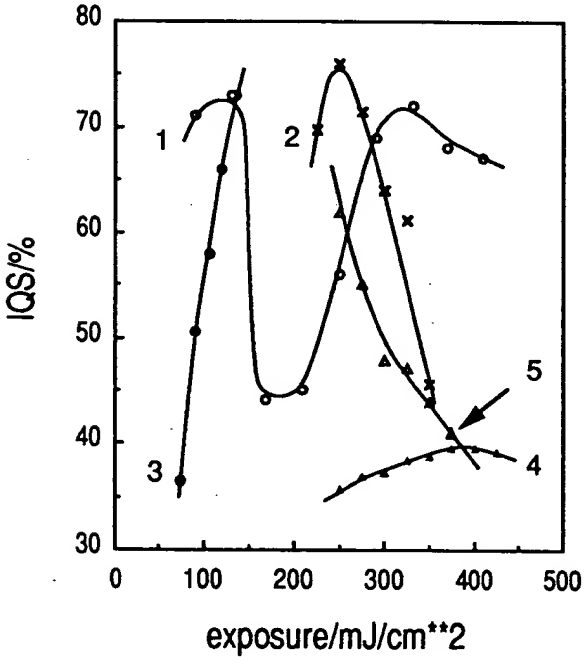

Figure 3b: IQS vs. exposure for various marker designs with PAS5000/50 and IX500, showing the exposure latitude for accurate focus measurement

- ▲ 0.6 µm duty grating
- △ 0.5 µm sub-divided fine grating (cleared surrounding area)
- × 0.32 µm sub-divided vertical fine grating
- ● 0.6 µm sub-divided fine grating (surrounding area chessboard like)
- ○ 0.6 µm fine grating (cleared surrounding area)

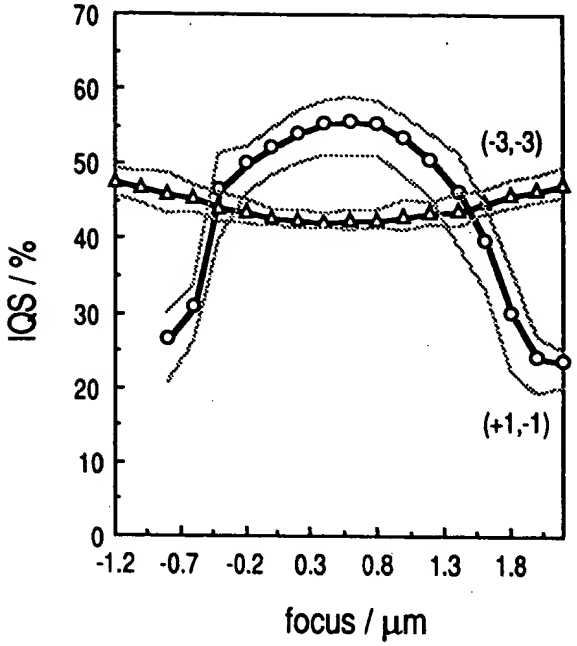

Figure 4. Reproducability of IQS vs. focus for fixed exposure (IQS±3*sigma limits) for markers of Fig. 2 for PAS5000/50 and IX500 on Si substrate (exposure for sub-divided fine grating marker (1,-1) is 80mJ/cm**2 and for duty marker (-3,-3) 450mJ/cm**2)

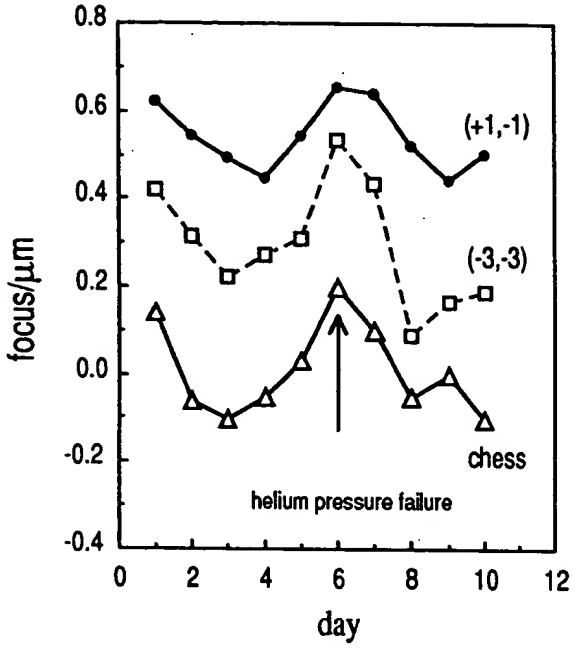

method	average focus	3-sigma
chess	0.11µm	0.48µm
(+1,-1)	0.54µm	0.23µm
(-3,-3)	0.29µm	0.42µm

Figure 5. Focus vs. time for PAS5000/50, measured by chessboard and ATS for the marker type of Fig. 2

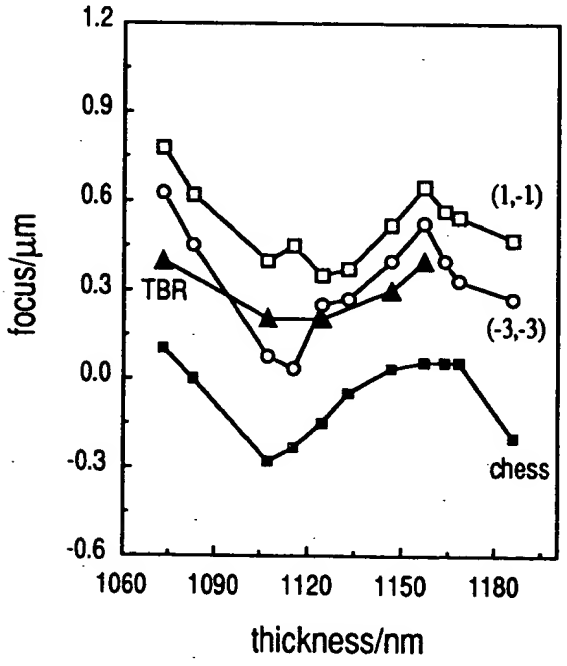

Figure 6. Focus vs. resist layer thickness for PAS5000/50 and IX500, determination with chessboard, SEM linewidth top-base-ratio measurement (TBR) and ATS for marker of Fig. 2

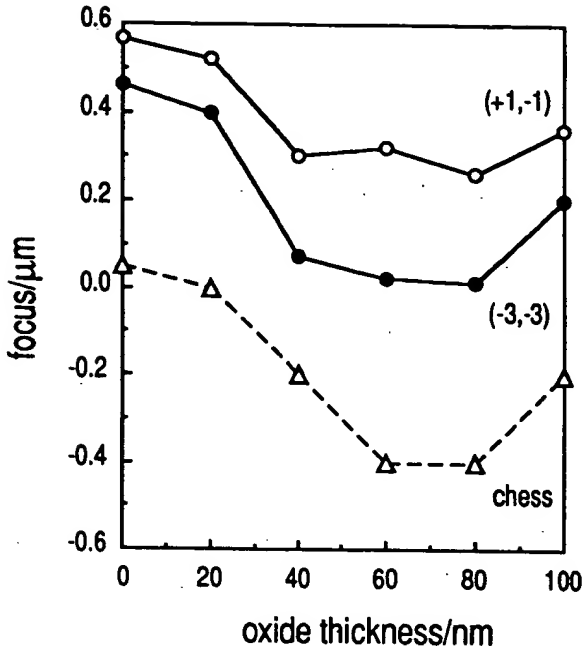

Figure 7a. Optimum focus vs. oxide thickness for substrate oxide, measured by PAS5000/50 and IX500/1.195µm with chessboard and ATS by markers of Fig. 2

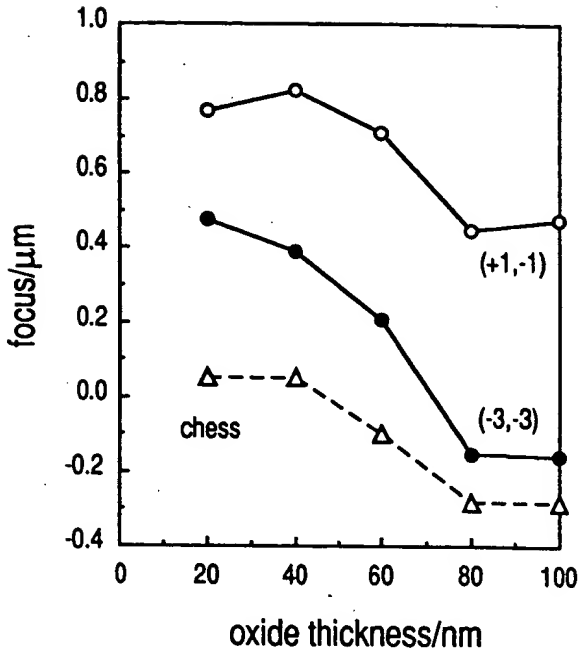

Figure 7b. same as Fig. 7a for substrate oxide/nitride (nitride thickness 200 nm)

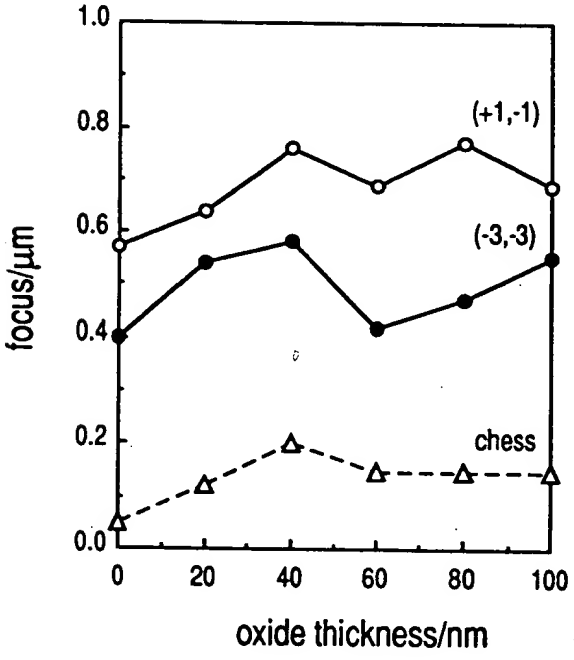

Figure 7c. same as Fig. 7a for substrate oxide/poly (poly thickness 300 nm)

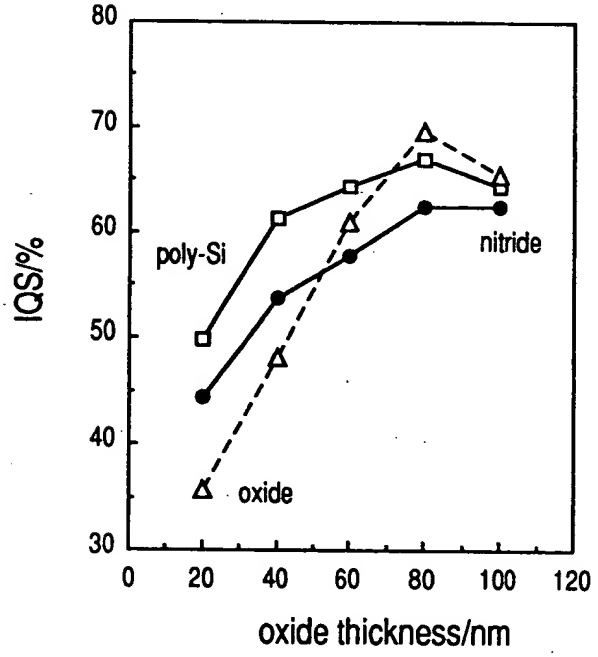

Figure 7d. IQS vs. oxide thickness for various substrates (oxide/poly, oxide/nitride, oxide), fixed exposure (85mJ/cm**2) and "best focus" case for marker (+1,-1)

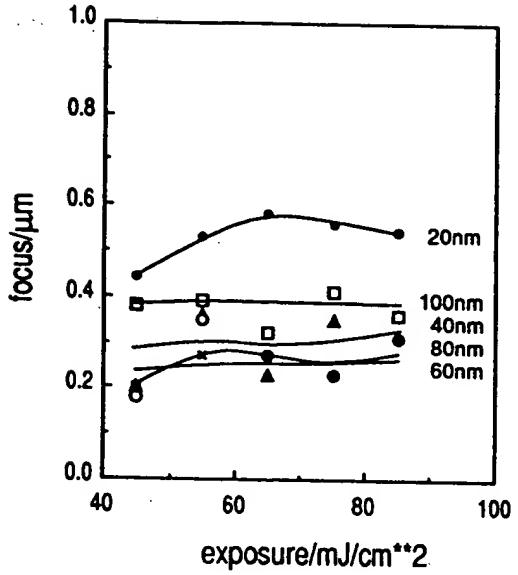

Figure 8. Optimum focus vs. exposure for marker (+1,-1) of Fig. 2, measured by ATS with PAS5000/50 and IX500 on substrate oxide for various oxide thicknesses

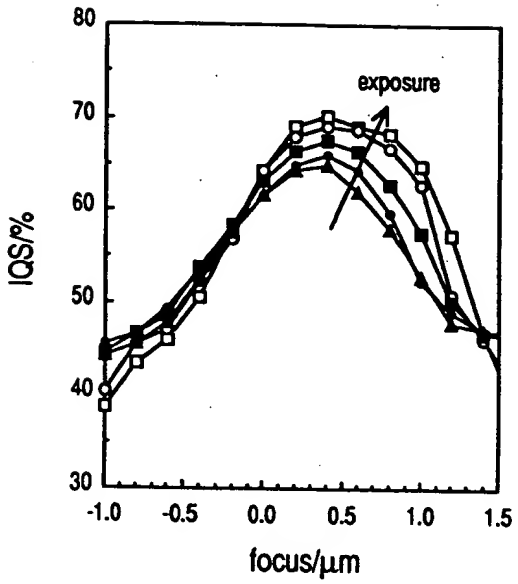

Figure 9. IQS vs. focus/exposure for PAS5000/70 and thinned McDermid resist (0.5µm), measured by ATS on developed pattern of a sub-divided fine grating marker (exposure range 30...90mJ/cm**2)

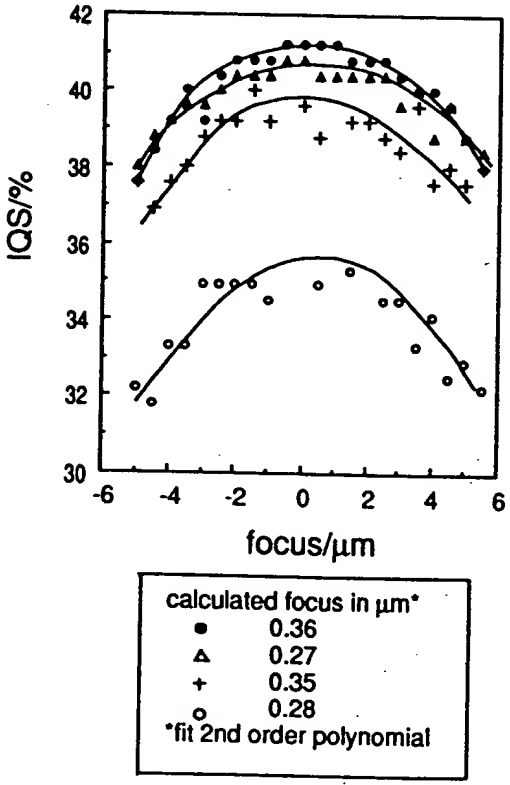

Figure 10a. IQS vs. focus/exposure for PAS5000 /50 and IX500, measured with ATS on ***latent image*** of a sub-divided fine grating marker on substrate AlSiCu

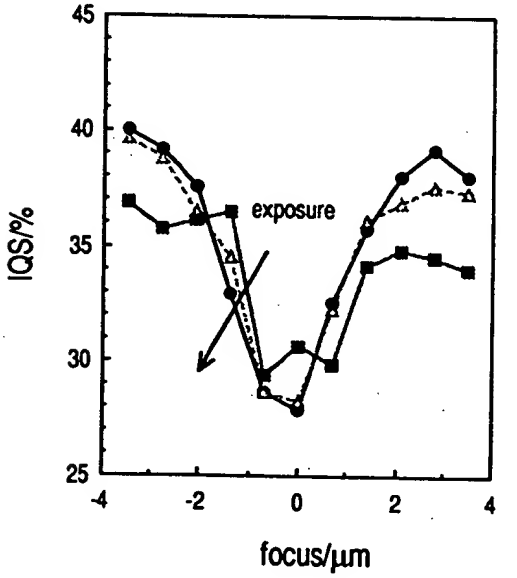

Figure 10b. IQS vs. focus/exposure for ASM-L's PAS5000/70 and Shipley's XP89131, measured by ATS on ***latent image*** (with PEB) of a "diffraction enhanced" (Moir'e grating) marker (exposure range 40...60mJ/cm**2)

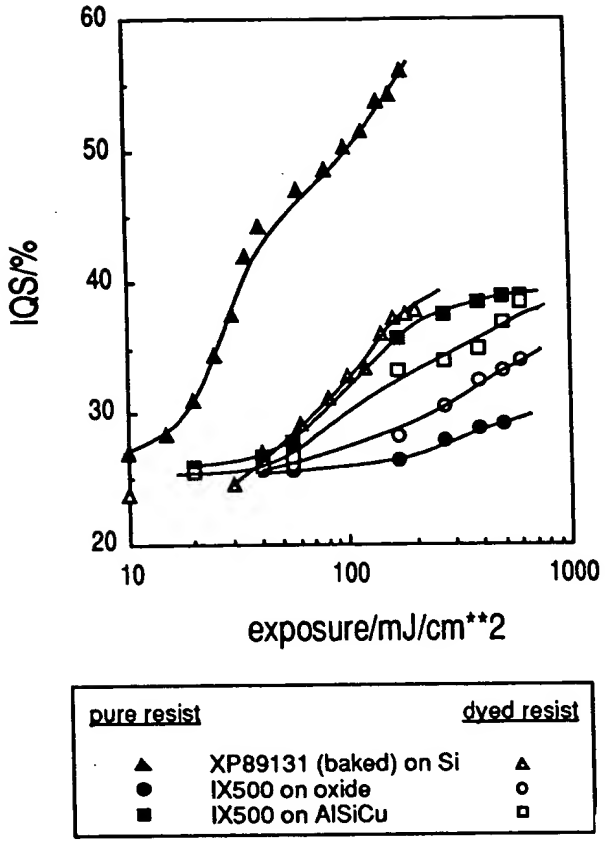

Figure 11. IQS vs. exposure of latent image of standard alignment marker in dyed and non-dyed IX500/JSR as well as XP89131/Shipley, measured withPAS5000/50 and /70

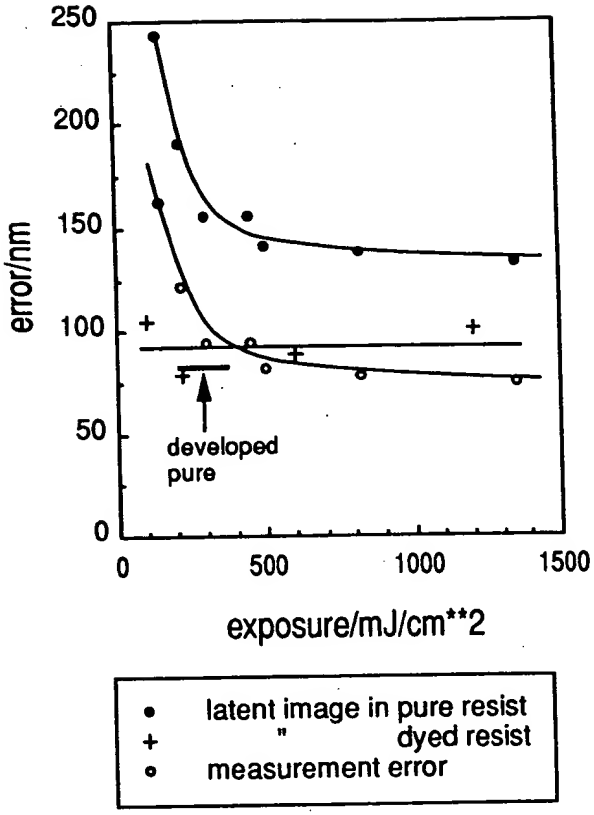

Figure 12. Overlay error [given as SQRT (3*Sx**2+3*Sy**2), Sx,y: sigma value] and (3-sigma) overlay measurement error vs. exposure, measured on latent image of standard marker in dyed and pure resist as well as on developed patterns with PAS 5000/50